Quantum coherence and entanglement in the avian compass

Erik Gauger*,[1] Elisabeth Rieper*,[2,†] John J. L. Morton,[1,3] Simon C. Benjamin,[2,1] and Vlatko Vedral[2,3,4]

[1] *Department of Materials, University of Oxford, Parks Rd, Oxford OX1 3PH, UK*
[2] *Center for Quantum Technologies, National University of Singapore, Singapore*
[3] *Clarendon Laboratory, University of Oxford, Parks Rd, OX1 3PU, UK*
[4] *Department of Physics, National University of Singapore, Republic of Singapore*

(Dated: September 30, 2009)

Tremendous efforts are underway to build technologies that harness the deep quantum phenomena of superposition and entanglement. These properties have proven fragile, often decaying rapidly unless cryogenic temperatures are used. Could life have evolved to exploit such phenomena [1]? Certain migratory birds have the ability to sense very subtle variations in the Earth's magnetic field [2]. Here we use recent experimental observations [3] together with the well developed 'radical pair' model of the avian compass [4], and employ a master equation with various decoherence operators in order to examine the system's vulnerability to environmental noise. Remarkably, the room temperature noise tolerance in this natural system appears greater than that of the best man-made molecular radical [5] or solid state singlet/triplet devices [6]. We find that entanglement, though probably not an essential feature of this process, appears to persist to tens of microseconds, or more.

Recently several authors have raised the intriguing possibility that living systems may use non-trivial quantum effects to optimise some tasks. Studies range from the role of quantum physics in photosynthesis [7, 8, 9, 10] and in natural selection itself [11], through to the observation that 'warm and wet' living systems can embody entanglement given a suitable cyclic driving [12]. In this letter, we examine a particularly important form of natural information processing known as magnetoreception – the ability to sense characteristics of the surrounding magnetic field. There are a several mechanisms by which this sense may operate [2]. In certain species (including some birds [4], fruit flies [13, 28] and even plants [14]), the evidence supports a Radical Pair (RP) mechanism, which relies on the quantum evolution of a spatially-separated interacting pair of electron spins. This is supported by results from the field of spin chemistry [15, 16, 17, 18, 19] and recent experiments which were able to demonstrate a chemical compass [20].

By manipulating a captive bird's magnetic environment and recording its response, one can make inferences about the mechanism of the magnetic sensor [3, 21, 22, 23]. Specifically, European Robins are only sensitive to the inclination and not the polarization of the magnetic field [21], and this sensor is evidently activated by photons entering the bird's eye [22]. Importantly for the present analysis, a very small oscillating magnetic field can disrupt the bird's ability to orientate [3, 23]. It is also significant that birds are able to 'train' to different field strengths, suggesting that the navigation sense is robust, and unlikely to depend on very special values for the parameter in the model [3].

All these experiments can be explained with the commonly-accepted Radical Pair (RP) model, see Fig.1. Here we employ the simplest RP model, considering the spins of two electrons [4, 24] and one nucleus of the molecule. Absorption of a photon and subsequent transfer of one electron to an acceptor part of the molecule, gives rise to a radical pair initially in the singlet state. Due to the spatial separation it now becomes meaningful to talk about electron spin entanglement. Because of the nuclear interaction with one of the electron spins, the singlet state is no longer an eigenstate of this Hamiltonian leading to an angle dependent singlet-triplet oscillation. Recombination occurs either from the singlet or triplet state, leading to different chemical endproducts. The concentration of those products constitutes a macroscopic chemical signal, correlated to the orientation of the

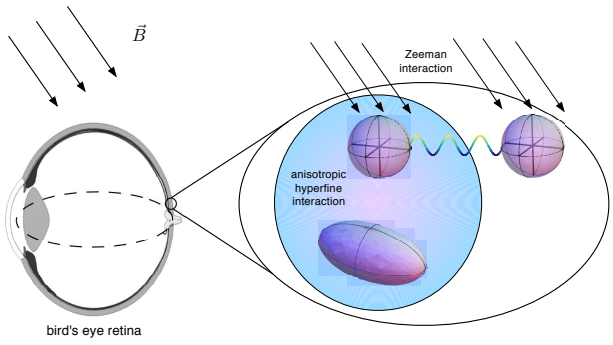

FIG. 1: Schematic of the bird's eye. The back of the eye contains numerous molecules [30], fixed with specific orientations but not necessarily ordered. In the simplest RP model, each such molecule involves three crucial components (see inset): there are two electrons, initially photo-excited to a singlet state, and a nuclear spin that couples to *one* of the electrons. This coupling is anisotropic, so that the molecule has a directionality to it.

*These authors have contributed equally to the work reported here.

molecule with the magnetic field.

We employ the Hamiltonian corresponding to the system once the two electrons have become separated. The anisotropic hyperfine tensor coupling the nucleus and electron 1, is conveniently written in its diagonal basis $A = \mathrm{diag}(A_x, A_y, A_z)$, and we assume an axially symmetric (or cigar-shaped) molecule with $A_z = 10^{-5}$ meV and $A_x = A_y = A_z/2$. This is the simplest assumption that can provide us with directionality, and we have chosen the general shape and magnitude of the tensor to be consistent with [29]. The Hamiltonian is

$$H = \hat{I} \cdot \mathbf{A} \cdot \hat{S}_1 + \gamma \mathbf{B} \cdot (\hat{S}_1 + \hat{S}_2),$$

where $\hat{I}$ is the nuclear spin operator, $\hat{S}_i = (\sigma_x, \sigma_y, \sigma_z)_i$ are the electron spin operators $(i = 1, 2)$, $\mathbf{B}$ is the magnetic field vector and $\gamma = \frac{1}{2}\mu_0 g$ the gyromagnetic ratio with μ_0 being Bohr's magneton and $g = 2$ the g-factor. The factor $1/2$ in the gyromagnetic ratio accounts for the fact that we have a spin one-half system, but we will use Pauli matrices such as $\sigma_z = \mathrm{diag}\{1, -1\}$ etc. Here only one electron is coupled to one nucleus, whereas the remote electron is so weakly interacting that we describe it as free. Previous authors have considered the case where more than one nucleus couples to the system [3, 19, 31], In the Supplementary Information we show our basic conclusions are not affected by varying the hyperfine tensor, adding a second nuclear spin, or even by replacing the term completely with a anisotropic electron g-factor.

Generally, the magnetic field we employ is

$$\begin{aligned} \mathbf{B} &= B_0(\cos\varphi \sin\vartheta, \sin\varphi \sin\vartheta, \cos\vartheta) \\ &+ B_{\mathrm{rf}} \cos\omega t(\cos\phi \sin\theta, \sin\phi \sin\theta, \cos\theta), \end{aligned} \quad (1)$$

where $B_0 = 47\ \mu$T is the Earth's magnetic field in Frankfurt [3], and the angles describe the orientation of magnetic field to the basis of the HF tensor. $B_{\mathrm{rf}} = 150$ nT is an additional oscillatory field only applied in our simulations where explicitly mentioned. For resonant excitation with the uncoupled electron spin, $\hbar\omega = 2\gamma B_0$, so that $\nu = \omega/(2\pi) = 1.316$MHz.

Because of the axial symmetry of the HF tensor we can set $\varphi = 0$ and focus on the ϑ in the range $[0, \pi/2]$ without loss of generality. Furthermore, for the oscillatory field, we set $\phi = 0$.

We model the dynamics of the system with a quantum master equation (ME) approach. We employ operators representing the relaxation processes; specifically, we include two 'shelving states' which represent the system having decayed either from an electron singlet state, or from one of the triplet states. Ultimately one of these two forms of relaxation will occur. The three spins span an 8 dimensional Hilbert space to which we therefore add two further levels $|S\rangle$ and $|T\rangle$ for the singlet and triplet decay outcomes, respectively. The populations of these levels will then correspond the singlet and triplet yield.

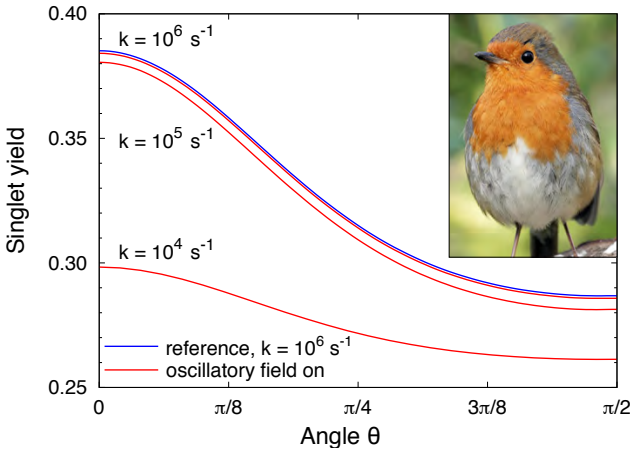

FIG. 2: **Angular dependence of the singlet yield in the presence of an oscillatory field.** The blue reference curve shows the singlet yield obtained in the Earth's magnetic field with $B_0 = 47\mu$T), which is independent of the decay rate k for $k \leq 10^7$ s^{-1}. For better visibility, the blue curve has been shifted upwards by 0.001. The red curves show the singlet field when a 150 nT magnetic field oscillating with a frequency resonant with the Zeeman splitting of the uncoupled electron (1.316 MHz) magnetic field is superimposed perpendicular to the direction of the static field. We see that this only has an appreciable effect on the singlet yield once k is of order 10^4 s^{-1}. Inset: a European Robin (© David Jordan)

With the usual definiton of singlet $|s\rangle$ and triplet states $|t_i\rangle$ in the electronic subspace, while $|\uparrow\rangle$ and $|\downarrow\rangle$ describing the states of the nuclear spin, we define the following decay operators:

$$\begin{aligned} P_{S,\uparrow} &= |S\rangle\langle s, \uparrow| \\ P_{T_0,\uparrow} &= |T\rangle\langle t_0, \uparrow| \\ P_{T_+,\uparrow} &= |T\rangle\langle t_+, \uparrow| \\ P_{T_-,\uparrow} &= |T\rangle\langle t_-, \uparrow| \end{aligned}$$

and similarly for the 'down' nuclear states. This gives us a total of two singlet projectors and six triplet projectors. For simplicity and because this choice corresponds exactly to the expression for singlet yield used in previous literature, all eight projectors have the same decay rate $\Gamma_P = k$.

For our model we start from a initial density matrix $\rho(0)$ corresponding to the electrons in a pure singlet state, and a completely mixed nuclear state, i.e.,

$$\rho(0) = id_n \otimes |s\rangle\langle s| = |s, \downarrow\rangle\langle s, \downarrow| + |s, \uparrow\rangle\langle s, \uparrow|.$$

The decay to the two shelving levels is then described using a standard quantum ME with above decay operators which effectively discrimate singlet and triplet decay events

$$\dot{\rho} = -\frac{i}{\hbar}[H, \rho]_- + k\left(\sum_{i=1}^{8} P_i \rho P_i^\dagger - \frac{1}{2}\left(P_i^\dagger P_i \rho + \rho P_i^\dagger P\right)\right) \quad (2)$$

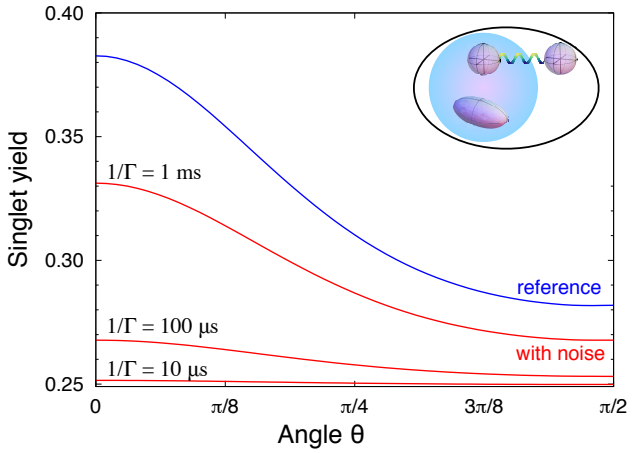

FIG. 3: **Angular dependence of the singlet yield in the presence of noise**. A) All curves were obtained using $k = 10^4$. The blue curve provides a reference in the absence of noise and the red curves show the singlet yield for different noise rates given. It is apparent from the plot that a noise rate $\Gamma > 0.1k$ has a dramatic effect on the magnitude and contrast of the singlet yield.

Note that Eqn.(2) does not contain any environmental noise, though this does not alter the estimates of the decay rate k (see Supp. Information). In the previous literature on the RP model of the avian compass, it has been common to employ a Liouville equation to model the dynamics. In fact, a term-by-term comparison of the evolution of the terms of the density matrix readily confirms that this former approach and our ME are exactly equivalent in the absence of environmental noise. Both agree with the singlet yield integral, $\Phi = \int_0^\infty \langle\psi^-|Tr_n(\rho(t))|\psi^-\rangle k e^{-kt} dt$, another commonly used quantity from the prior literature, when singlet and triplet reaction rates are equal. Specifically, the ultimate population of our singlet 'shelf' $|S\rangle$ then corresponds to Φ. However, when we presently wish to introduce various kinds of noise operator, in particular the pure phase variant, then the ME approach provides a more intuitive framework.

We now wish to determine an appropriate choice for our parameter k in Eqn. 2. In Ref. 3, the authors report that a perturbing magnetic field of frequency of 1.316 MHz (i.e. the resonance frequency of the 'remote' electron) can disrupt the avian compass. They note that this immediately implies a bound on the decay rate (since the field would appear static for sufficiently rapid decay). Here we aim to refine this bound on k by considering the oscillating magnetic field *strength* which suffices to completely disorient the bird's compass, i.e. 150 nT. (Indeed, even a 15 nT field was reported as being disruptive, but to be conservative in our conclusions we take the larger value here.) To model this effect, we activate the oscillatory field component defined in Eqn. 1 and examine the singlet yield (i.e. the eventual population of shelving state $|S\rangle$) as a function of the angle between the Earth's field and the molecular axis. Consistent with the experimental work, we find that there is no effect at such weak fields when the oscillatory field is parallel to the Earth's field. Therefore for our analysis we set the oscillatory field to be perpendicular. The results are shown in Figure 2. We conclude that if the oscillating field is to disorient the bird, as experiments showed, then the decay rate k should be approximately 10^4 s^{-1} or less. For higher values of k (shorter timescales for the overall process) there is no time for the weak oscillatory field to significantly perturb the system; it relaxes before it has suffered any effect. Such a value for the decay rate is consistent with the long RP lifetimes in certain candidate cryptochrome molecules found in migratory birds [25].

Taking the value $k = 10^4$ s^{-1}, we are able to move to the primary question of interest: how robust this mechanism is against environmental noise. There are several reasons for dehorence. For example dipole interaction, electron-electron distance fluctuations and other particles' spin interaction with the electrons will cause decoherence. We describe generic environmental noise with a standard Lindblad ME technique [26], where Eqn. 2 above is extended with a dissipator as follows:

$$\dot{\rho} = \begin{matrix}\text{RHS of} \\ \text{Eqn.2}\end{matrix} + \sum_i \Gamma_i \left(L_i \rho L_i^\dagger - \frac{1}{2}\left(L_i^\dagger L_i \rho + \rho L_i^\dagger L_i \right) \right) \quad (3)$$

Noise operators L_i are σ_x, σ_y, σ_z for each electron spin individually (i.e. tensored with identity matrices for the nuclear spin and the other electron spin). This gives a total of six different noise operators L_i and we use the same decoherence rate Γ for all of them. We are now in a position to determine the approximate level of noise which the compass may suffer, by finding the magnitude of Γ for which the angular sensitivity fails. This is shown in Fig. 3. Conservatively, we can say that when $\Gamma \geq k$, the angular sensitivity is highly degraded. This is remarkable, since it implies the decoherence time of the two-electron compass system is of order 100 μs or more [32]! To provide context for this number, we note that the best laboratory experiment involving preservation of a molecular electron spin state has accomplished a decoherence time of $80\mu s$ [5].

It is interesting to ask, what is the significance of entanglement between the spins in the avian compass? Having inferred approximate values for the key parameters, we can plot an appropriate entanglement measure over the course of the process, from the initial singlet generation to the eventual decay. The metric we use is negativity:

$$N(\rho) = \frac{||\rho^{T_A}||}{2}$$

where $||\rho^{T_A}||$ is the trace norm of the partial transpose of the system's density matrix. The transpose is applied

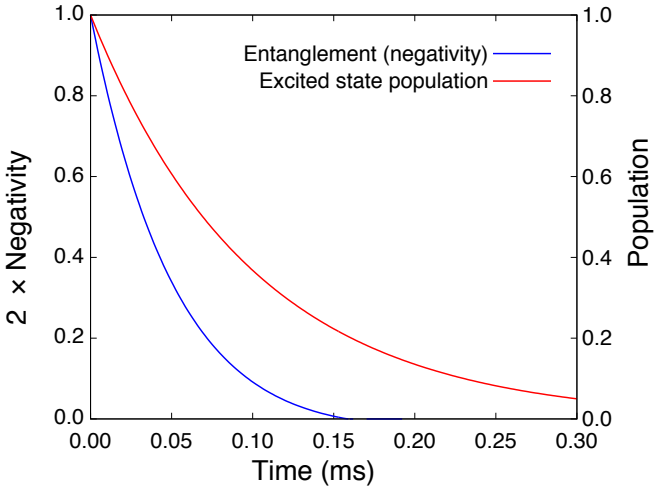

FIG. 4: A plot indicating the decline and disappearance of entanglement in the compass system, given the parameter k and the noise severity Γ defined above. Here the angle between the Earth's field and the molecular axis in $\pi/4$, although the behavior at other angles is similar. The entanglement metric is negativity as defined in the text.

to the uncoupled electron, thus performing the natural partitioning between the electron, on one side, and the coupled electron plus its nucleus, on the other. Fig. 4 shows how this negativity evolves under our noise model. Clearly, the initial singlet state is maximally entangled. Under noise, entanglement falls off at a faster rate than the decay of population from the excited state.

The noise model above is of the most general kind, representing a unrestricted degradation of the system's state due to environmental interactions. We further have found that the compass mechanism is almost immune to pure phase noise (typically the most aggressive noise in artificial systems). Even starting from a fully dephased state $(|s\rangle\langle s| + |t_0\rangle\langle t_0|)/2$, the compass operates well. However, in the Supplementary Information we show that if such noise were naturally present at a high level in the compass (exceeding the generic noise level Γ by more than an order of magnitude) then it would render the bird immune to the weak oscillatory magnetic fields of Ref. [3]. Thus the sensitivity to oscillatory fields implies that both amplitude and phase, and thus entanglement, are indeed protected within the avian compass on timescales exceeding tens of microseconds. It is not clear *why* such remarkable protection occurs, but given the widely-accepted RP model together with the recent experimental data [3], this conclusion follows.

We thank Earl Campbell, Chris Rodgers, Peter Hore and Kiminori Maeda for stimulating discussions. We thank the National Research Foundation and Ministry of Education of Singapore for support. EMG acknowledges support from the Marie Curie Early Stage Training network QIPEST (MEST-CT-2005-020505) and the QIPIRC (No. GR/S82176/01) for support. JJLM and SCB thank the Royal Society for support. JJLM thanks St. John's College, Oxford. VV acknowledges financial support from the Engineering and Physical Sciences Research Council, the Royal Society and the Wolfson Trust in UK.

We note that in the final stages of preparation of this manuscript, a related work has appeared which considers a chemical magnetometer in the context of quantum control [27].

† Electronic address: elisabeth.rieper@quantumlah.org

[1] P. C. W. Davies: *Does quantum mechanics play a non-trivial role if life*, BioSystems **78** , 69-79, (2004).
[2] S. Johnsen, K. J. Lohmann: *Magnetoreception in animals*,Physics Today, (2008).
[3] T. Ritz et al.: *Magnetic Compass of Birds Is Based on a Molecule with Optimal Directional Sensitivity*, Biophysical Journal, **96** 3451-3457, (2009).
[4] T. Ritz, S. Adem, K. Schulten:*A Model for Photoreceptor-Based Magnetoreception in Birds*, Biophysical Journal **78**, 707-718, (2000).
[5] J. J. L. Morton et al.: *Electron spin relaxation of $N@C_{60}$ in CS_2*, J. Chem. Phys. **124**, 014508, (2006).
[6] J. R. Petta et al.: *Coherent Manipulation of Coupled Electron Spins in Semiconductor Quantum Dots*, Science **309** 2180-2184, (2005).
[7] G. S. Engel et al.: *Evidence for wavelike energy transfer through quantum coherence in photosynthetic systems*, Nature **446**, 782-786 (2007).
[8] M. Mohseni, P. Rebentrost, S. Lloyd, A. Aspuru-Guzik: *Environment-assisted quantum walks in photosynthetic energy transfer*, J. Chem. Phys. **129**, 174106, (2008).
[9] M.B. Plenio, S.F. Huelga: *Dephasing assisted transport: Quantum networks and biomolecules*, New. J. Phys. **10**, 113019 (2008).
[10] M. Sarovar, A. Ishizaki, G. R. Fleming, K. Birgitta Whaley, *Quantum entanglement in photosynthetic light harvesting complexes*, arXiv: 0905.3787, (2009).
[11] S. Lloyd: *A quantum of natural selection*, Nature Physics **5**, 164, (2009).
[12] J.-M. Cai, S. Popescu, H. J. Briegel:*Dynamical entanglement in oscillating molecules*, arXiv:0809.4906, (2008).
[13] R. J. Gegear, A. Casselman, S. Waddell, S. M. Reppert: *Cryptochrome mediates light-dependent magnetosensitivity in Drosophila*, Nature **454**, 1014 (2008).
[14] M. P. Galland, T. Ritz, R. Wilschko, and W. Wilschko:*Magnetic intensity affects cryptochrome-dependent response in Arabidopsis thaliana*, Planta. **225**, 615 (2006).
[15] C. R. Timmel, K. B. Henbest: *A study of spin chemistry in weak magnetic fields*, Phil Trans Roy Soc London A **362**, 2573-2589, (2004).
[16] Y. Liu et al.:*Magnetic field effect on singlet oxygen production in a biochemical system*,Chem.Commun., 174-176, (2005).
[17] T. Miura, K. Maeda, T. Arai: *The Spin Mixing Process of a Radical Pair in Low Magnetic Field Observed by Transient Absorption Detected Nanosecond Pulsed Magnetic*

Field Effect, J. Phys. Chem. A **110**, 4151-4156, (2006).
[18] C. T. Rodgers: *Magnetic Field Effects in Chemical Systems*, Pure Appl. Chem., **81**, No.1, 87-111, (2009).
[19] C. T. Rodgers, P.J. Hore: *Chemical magnetoreception in birds: The radical pair mechanism*, PNAS, **106** 2, 353-360, (2009).
[20] K. Maeda et al.:*Chemical compass model of avian magnetoreception*, Nature, **453**, 387, (2008).
[21] W. Wiltschko, R. Wiltschko: *Magnetic compass of European robins* Science, **176**, 6264, (1972).
[22] W. Wiltschko, R. Wiltschko: *Magnetic compass orientation in birds and its physiological basis* Naturwissenschaften, 89:445-452, (2002).
[23] T. Ritz, P. Thalau, J.B. Philips, R. Wiltschko, W. Wiltschko:*Resonance effects indicate a radical-pair mechanism for avian magnetic compass*, Nature, **429**, 177, (2004).
[24] K. Schulten, C. E. Swenberg, A. Weller,*A biomagnetic sensory mechanism based on magnetic field modulated coherent electron spin motion*, Z. Phys. Chem. **NF111**, 1, (1978).
[25] Liedvogel et al.:*Chemical Magnetoreception: Bird Cryptochrome 1a Is Excited by Blue Light and Forms Long-Lived Radical-Pairs*, PLoS ONE, **10** e1106, (2007).
[26] M. A. Nielsen and I. C. Chuang *Quantum Computation and Quantum Information, Cambridge* Cambridge University Press (2000).
[27] J.-M. Cai, G. G. Guerreschi, H. J. Briegel: *Quantum control and entanglement in a chemical compass* , arXiv:0906.2383, (2009).
[28] T. Yoshii, M. Ahmad, C. Helfrich-Forster: *Cryptochrome Mediates Light-Dependent Magnetosensitivity of Drosophila's Circadian Clock*,Plos One (2009).
[29] O. Efimova, P. J. Hore:*Evaluation of nuclear quadrupole interactions as a source of magnetic anisotropy in the radical pair model of the avian magnetic compass*, Molecular Physics, **107**, 665-671 (2009).
[30] I. A. Solov'yov, K.Schulten: *Magnetoreception through Cryptochrome May Involve Superoxide*, Biophysical Journal, **96**, 4804 - 4813 (2009).
[31] C.T. Rodgers:*Magnetic Field Effects in Chemical Systems*, PhD Thesis, Oxford (2007).
[32] One could assume the bird to be more easily perturbed by the oscillatory field (Fig. 2), and obtain a larger k. However, that same assumption of high sensitivity should then be applied to the noise analysis (Fig. 3) and in fact the two assumptions would cancel to give the same basic estimate for the decoherence rate. This cancellation is robust, being valid over an order of magnitude in k.

Supporting Material

THE TERMINOLOGY AND TECHNIQUES USED IN THE MANUSCRIPT

The terminology used in the main paper arises from the foundations of quantum mechanics and has more recently become important in the field of quantum information (QI). Thus we describe the avian compass and its dynamics in terms of quantum coherence, environmental decoherence, and entanglement; moreover we use the quantum master equation technique to model the system's dynamics. These terms and techniques are rather different to those of the established radical pair (RP) and avian compass communities, therefore it is appropriate to justify their use and relate them to the established terminology.

The primary conclusion of the paper concerns the extent to which quantum coherence is protected in the compass system. By this term, we refer to the *purity* of the system, which is degraded by interactions with the environment because these will generally act as a kind of measurement of the state (for example, by taking a quantum of energy from the state and thus leaving it in a specific low-energy state). Since the 'outcome' of this measurement is lost to the environment, the system's state becomes a *mixture* of the multiple possible states – generically this loss of purity is called decoherence.

In the applied QI field, much effort is dedicated to the preservation of quantum coherence. In order for quantum coherence to be maintained, it is essential to prevent all kinds of interaction, including those that would *flip* spins, allowing them to relax and lose energy, and also those interactions which would merely alter the *phase* relationships in the state (dephasing noise). Thus while the concept of *spin relaxation* is a typical signature of general coupling to the environment, we must also examine the effect of pure phase noise; the latter alone can suffice to completely degrade a pure state such as the singlet $|s\rangle$ into a completely incoherent mixture of $|s\rangle$ and $|t_0\rangle$ and would therefore undermine our conclusion. In order to examine this point, and establish whether full coherence is indeed maintained, it is necessary to construct a equation for the dynamics of the system where pure phase noise alone occurs. This is most naturally done with the quantum master equation (QME) formalism and the corresponding Lindblad noise operators – however, it is important to note (as mentioned in the main paper) that the QME is actually identical to the more conventional Liouville equation in the case of zero environmental noise. We select the QME as the most suitable tool for examining specific decoherence models, including both general spin relaxation and those that specifically cause only dephasing.

Finally we note that, because the RP involves two electrons, and these are spatially separated, it is meaningful to use the quantity 'entanglement' as one specific characterization of their mutual state. The established avian compass literature would tend to refer to the related concept of *spin correlation*, however, entanglement is subtly and importantly different in that it captures precisely the non-classical correlations between spins – it is impossible, for example, to create entanglement between two sites simply by exchanging classical information as to how the spins should be prepared. We chose to plot the entanglement in the avian compass because it is a key quantity (arguably, *the* essential quantity) in the quantum mechanics, and therefore a reader from that community will naturally wonder about this aspect. However, we find that while entanglement does persist for a remarkably long time, this is likely to be merely an implication of the long coherence time rather than a key property of the compass mechanism.

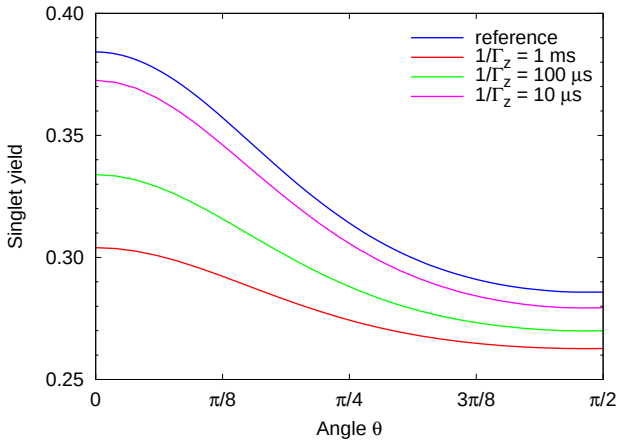

FIG. 5: Angular dependence of the singlet yield at $k = 10^4$ s^{-1} in the presence of the oscillatory field for different pure dephasing rates Γ_z. This is to be compared with the $k = 10^4$ s^{-1} line in Fig. 2 of the main paper. See text for an explanation.

SENSITIVITY TO OSCILLATORY FIELD IN THE PRESENCE OF PURE DEPHASING

Interestingly, if we begin the simulation with a completely dephased state: $(|s\rangle\langle s| + |t_0\rangle\langle t_0|)/2$, the classical correlations are still sufficient for achieving adequate angular visibility and neither quantum phase coherence nor entanglement seems to be a prerequisite for the efficiency of the avian compass.

To explore this idea further, we would like to study 'pure dephasing' occurring *during* the singlet-triplet interconversion. In essence we use energy conserving noise operators, Eqn. (4), which are known to be the dominant source of decoherence in so many other artificially made quantum systems. By applying this specific noise, we confirm that the compass mechanism's performance is essentially immune, while of course the coherence of the quantum state of the electrons would be degraded.

One might be inclined to conclude that, if pure dephasing noise is indeed dominant, then the avian compass need not protect quantum coherence for the long time scales suggested in the main paper. But crucially, we also show that if such noise were naturally present at a high level in the compass (exceeding the generic noise level Γ by more than an order of magnitude) then it would render the bird immune to the weak oscillatory magnetic fields studied by Ritz *et al.* [1]. Thus the sensitivity to oscillatory fields implies that both amplitude and phase, and thus entanglement, are indeed protected within the avian compass on timescales exceeding tens of microseconds.

Since the electron spin singlet state is not an eigenstate of the Hamiltonian, the dephasing operators will be different from the ones mixing the phase of the singlet and triplet state within the electronic subspace. Instead, we replace the previously defined noise operators of L_i of Eq. (3) by appropriate dephasing operators as follows: we treat the remote electron and the eletron nuclear spin subsystem separately. Within both subsystems, we define dephasing operators

$$\begin{aligned} Z_i &= \frac{1}{\sqrt{2}}\left(\sum_{j\neq i}|\lambda_j\rangle\langle\lambda_j| - |\lambda_i\rangle\langle\lambda_i|\right) \\ &= \frac{1}{\sqrt{2}}\left(I_4 - 2|\lambda_i\rangle\langle\lambda_i|\right), \end{aligned} \tag{4}$$

where $\{|\lambda_i\rangle\}$ are the set of normalised eigenvectors of this subsystem. This results in two dephasing operators for the remote electron (these can be combined to a single σ_z operator rotated with the field) and four operators for the eletron nuclear spin subsystem. Each of these dephasing operators corresponds to fluctuations of one of the (subsystem's) energy levels.

Strikingly, the singlet yield is entirely unaffected by this particular kind of noise, i.e. it is entirely independent of the dephasing rate Γ_z. Thus, a curve obtained with this model coincides perfectly with the reference curve of Fig. 3 of the main paper. However, we show in the following that the dephasing rate of this model can be at most ten times faster than the generic noise rate to retain sensitivity to the oscillatory field.

Fig. 5 shows the singlet yield as a function of θ for different pure dephasing rates Γ_z. Pure phase noise would actually *protect* the compass from the harmful effect of an applied oscillatory field (by suppressing the Rabi oscillations caused by such a field). We see that an aggressive pure dephasing rate of $1/\Gamma_z = 10$ μs almost completely recovers the reference curve (corresponding to a noise-free system without oscillatory field).

GENERALITY OF THE MODEL

European robins can adjust to different strengths of the magnetic field. This implies, that their chemical compass cannot depend on the absolute value of the the electron spins hyperfine (HF) coupling. We here argue that the conclusion presented in the main paper is not only robust against variations in the field strength, but also does not depend on the specifics of the anisotropic interaction between electron 1 and its local environment. (Of the two electrons constituing the RP, only one of them can be significantly coupled to nuclear spin(s) because the resonance effect [1] occurs at exactly the frequency of the Zeeman splitting of an *unperturbed* electron.)

'Disc-shaped hyperfine tensor'

We have explicitly checked that our conclusions do not rely on the specifics of the HF tensor given in the main text. Specifically neither a weaker or stronger coupling, nor a different HF tensor symmetry changes our observations about the shortest time scale required for the process to be sensitive to the oscillatory field. Neither do these factors change the maximal tolerable environmental noise rates to maintain a pronounced signal contrast.

Here we describe one of the variants we have studied: a 'disc-shaped' HF-coupling tensor with coupling strengths that are different from the ones presented in the main paper. The largest coupling here is half as strong as the one presented in the text: $A_x = 0.5 \times 10^{-5}$ meV, $A_y = A_x/6, A_z = A_x$.

Fig. 6 shows that we obtain exactly the same qualitative behaviour as for the parameters used in the main text, the only difference being in the different shape of the singlet yield curve (as expected for a different geometry of HF tensor). The oscillatory field does not have an influence on the singlet yield for $k > 10^4$ s^{-1}, while a noise rate of $\Gamma > 0.1k$ leads to a dramatic reduction of contrast.

Anisotropic g-factor

Instead of coupling to nuclear spin(s), an anisotropic g-factor for one of the electrons could also lead to a singlet yield with an angular dependence [2]. We here show that our main conclusion remains valid under this different Hamiltonian of the RP.

For illustration purposes, we consider a prounounced anisotropy: the g-factor in z-direction is 0.8×2, i.e. 80% of the free electronic g-factor of $g = 2$, while in x and y-direction we have 0.3×2. A smaller anisotropy works as well, but gives less overall signal contrast (even in the unperturbed) scenario. We present results for these parameters in Fig. 7, confirming that the qualitative behaviour is still the same under these assumptions.

Markovian noise model

The noise model we employ is Markovian, implying that the information lost to the environment will not return to the system (as it would, wholly or partially, if the environment was entirely constituted by other isolated qubits that could effectively act as a memory). This Markovian assumption is the natural choice to make for a room temperature system whose detailed structure and environmental interactions are unknown. One can immediately think of 'likely suspects' for decoherence in the present system that would be Markovian: for example, modulation in the electron-electron separation due to vibrations in the supporting matrix. But more importantly, while one can reasonably speculate that there may *also* be non-Markovian processes occuring, between the core system and other degrees of freedom that are well isolated from the true 'bath' degrees of freedom, this does not undermine our result. In essence, one would 'draw a dotted line' around the larger system, comprised of the core electron pair *together* with the non-Markovian environment, calling *that* the avian compass (although noting that only the core part plays an active role). One would conclude that this larger system is, again, remarkably well insulated from the environment.

RP PAIR MODEL WITH 2 NUCLEAR SPINS

In the model described in the main paper, there is a single nuclear spin coupled to one of the electrons. However, previous publications have studied the case where more than one nuclear spin is present [1, 3, 4]. Therefore, it is interesting to check whether the addition of a nuclear spin will alter our conclusions. The Hamiltonian now gains an additional coupling term,

$$H = \hat{I}_1 \cdot \mathbf{A}_1 \cdot \hat{S}_1 + \hat{I}_2 \cdot \mathbf{A}_2 \cdot \hat{S}_1 + \gamma \mathbf{B} \cdot (\hat{S}_1 + \hat{S}_2),$$

where $\mathbf{A}_1$ is the HF tensor of the main text and $\mathbf{A}_2 = 2/3\mathbf{A}_1$. Here we choose a second rugby shaped HF tensor oriented parallel to the first. Note that we have also considered different relative coupling strengths and geometries (such as a pancake shaped and rugby shaped tensor), but again, these choices do not influence our core conclusions. Results for the particular choice of parameters described above are shown in Fig. 8.

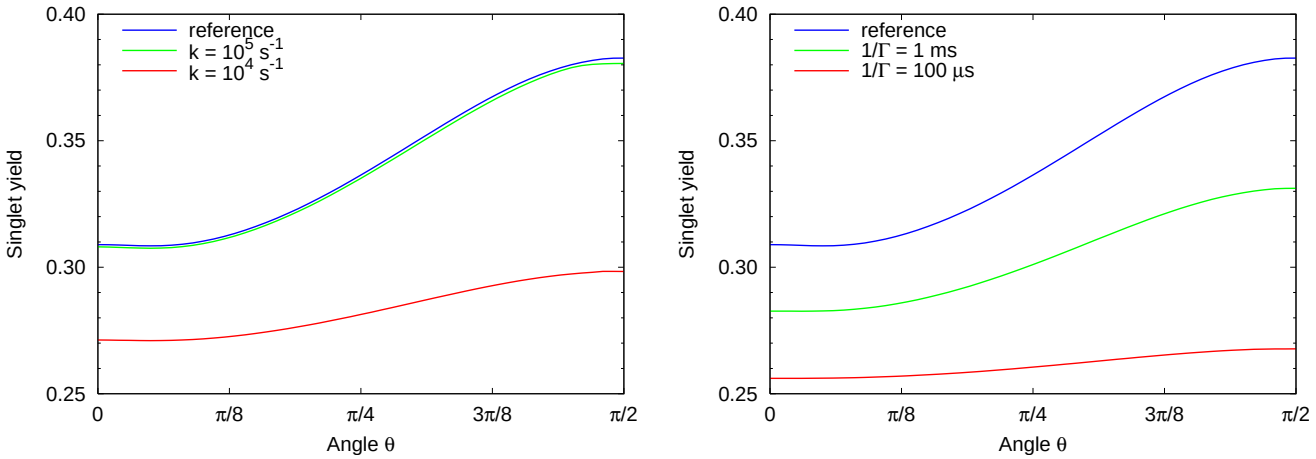

FIG. 6: Results for a disc-shaped HF tensor. The graph on the left is precisely analogous to Fig. 2 of the main text, showing angular dependence of the singlet yield in the presence of the oscillatory field for different decay rates k. The graph on the right corresponds to Fig. 3 of the main paper, showing angular dependence of the singlet yield in the presence of environmental noise [obtained with Eq. (5)] for different noise rates Γ. Although the curve shapes differ, the levels of contrast are the almost the same as the 'cigar' shaped HF model in the main paper.

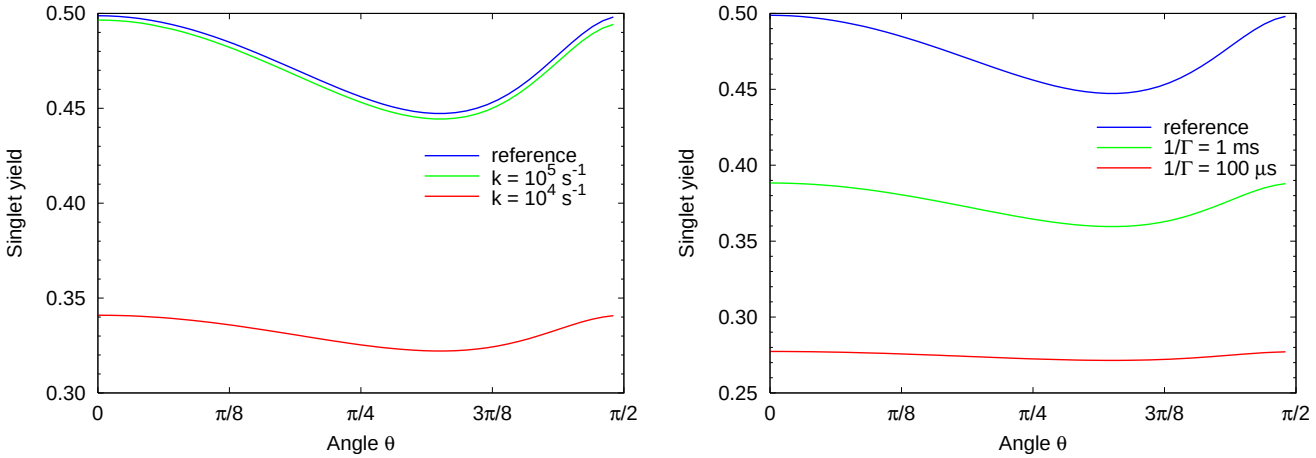

FIG. 7: Results for a model in which an anisotropic g-factor replaces the role of the nucleus to break the RP symmetry. The graph on the left is precisely analogous to Fig. 2 of the main text, showing angular dependence of the singlet yield in the presence of the oscillatory field for different decay rates k. The graph on the right corresponds to Fig. 3 of the main paper, showing angular dependence of the singlet yield in the presence of environmental noise for different noise rates Γ. Although the curve shapes differ, remarkably the levels of contrast remain similar to those of the conventional model in the main paper.

OSCILLATORY FIELD SENSITIVITY IN THE PRESENCE OF NOISE

In the first stage of the argument in the main paper, we show how the bird's sensitivity to field angle is degraded by an applied oscillatory field (Fig. 2, main paper). There we set the environmental noise operators to zero – this is of course unrealistic, and one might worry that finite noise could ultimately lead to less dramatic conclusions regarding protection of quantum coherence. However, here we show that the reverse is true: the addition of finite noise leads to a suppression of the harmful effect of the oscillatory field, and thus would lead one to infer a still more dramatic coherence time. Therefore, by setting the noise to zero we make the more conservative assumption.

We confirm this by employing the following master equation (which is exactly Eq. (3) of the main paper),

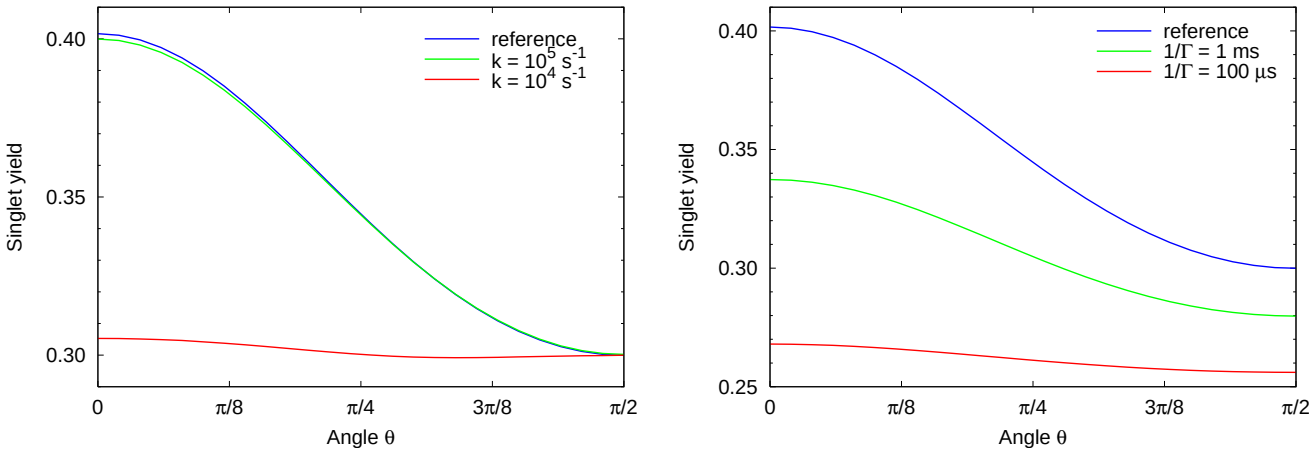

FIG. 8: Results for two nuclear spins coupled to electron 1. The graph on the left is precisely analogous to Fig. 2 of the main text, showing angular dependence of the singlet yield in the presence of the oscillatory field for different decay rates k. The graph on the right corresponds to Fig. 3 of the main paper, showing angular dependence of the singlet yield in the presence of environmental noise for different noise rates Γ. Although the curve shapes differ somewhat, nevertheless the parameters corresponding to serve degradation remain the same as those in the main paper ($k = 10^4$ s^{-1}, $\Gamma = 100$ μs).

while at the same time applying the oscillatory field:

$$\dot{\rho} = -\frac{i}{\hbar}[H,\rho] + k\left(\sum_{i=1}^{8} P_i\rho P_i^\dagger - \frac{1}{2}\left(P_i^\dagger P_i\rho + \rho P_i^\dagger P_i\right)\right) + \sum_{i=1}^{6}\Gamma_i\left(L_i\rho L_i^\dagger - \frac{1}{2}\left(L_i^\dagger L_i\rho + \rho L_i^\dagger L_i\right)\right). \quad (5)$$

The left panel of Fig. 9 corresponds to Fig. 2 of the main paper with such *additionally* applied noise at a rate of $\Gamma = 0.1k$. Note that the noise rate is adjusted with k, as we wish to concentrate on the combined effect of the oscillatory field and 'mild noise' over the timescale of the process. We infer that the singlet yield contrast is only significantly reduced when $k < 10^5$ s^{-1}, meaning the addition of noise to Fig. 2 in the main paper does not influence our conclusion.

To establish that this conclusion is robust with respect to the particular choice of $\Gamma = 0.1k$, we now investigate *different* noise rates for a fixed value of $k = 10^5$ s^{-1}. In the right panel of Fig. 9, we show a pair of curves for each noise rate: one obtained with and one without the oscillatory field. We make two observations: firstly, the two curves of each pair nearly coincide, indicating that there is only a small sensitivity to the oscillatory field indepedent of the noise rate. Secondly, the sensitivity *decreases* even more when the system is subjected to more aggressive noise.

In fact, this second observation is not surprising: we would not expect the additional noise terms to lead to a greater sensitivity to the oscillatory field. The singlet yield signal is corrupted by spin flips of the remote electron in the presence of the oscillatory field, which essentially causes the spin to Rabi flop, thus requiring quantum coherence. Therefore, any noise acting on the remote electron will decohere the spin and thus suppress rather than enhance the effect of the oscillatory field. This can also be seen in the right panel of Fig. 9: the red curves are very similar but not quite identical, the agreement is better for the green curves and almost perfect for the blue one.

† Electronic address: elisabeth.rieper@quantumlah.org

[1] T. Ritz et al.: *Magnetic Compass of Birds Is Based on a Molecule with Optimal Directional Sensitivity*, Biophysical Journal, **96** 3451-3457, (2009).

[2] I.A. Solov'yov, D. E. Chandler, K. Schulten:*Magnetic Field Effects in Arabidopsis thaliana Cryptochrome-1*, Biophysical Journal, **92**, 2711-2726 (2007).

[3] C. T. Rodgers, P.J. Hore: *Chemical magnetoreception in birds: The radical pair mechanism*, PNAS, **106** 2, 353-360, (2009).

[4] C.T. Rodgers:*Magnetic Field Effects in Chemical Systems*, PhD Thesis, Oxford (2007).

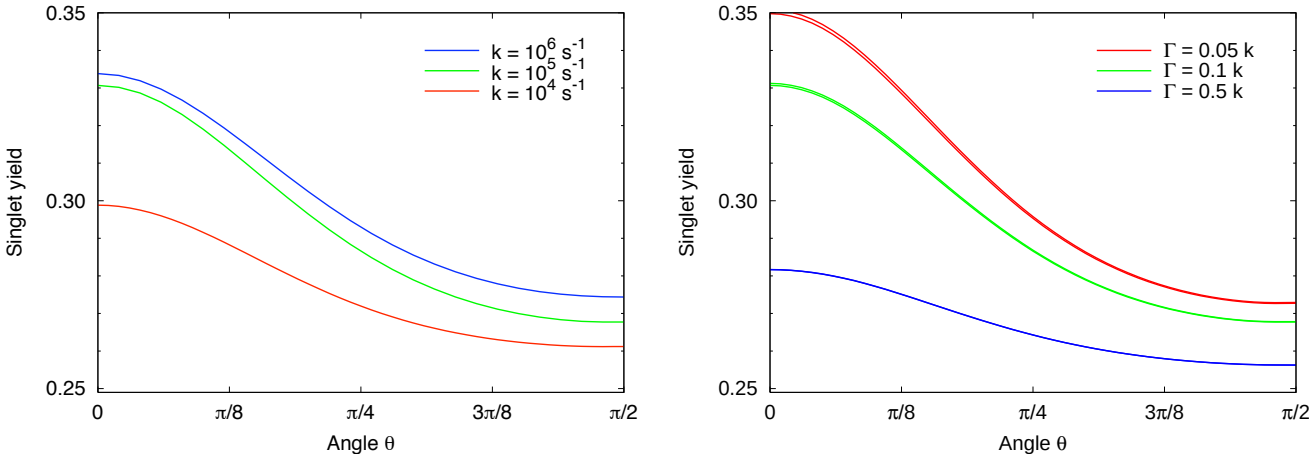

FIG. 9: **Left:** singlet yield as a function of θ in the presence of the resonant oscillatory field with additionally applied noise at a rate $\Gamma = 0.1k$ (see text). **Right:** The singlet yield as a function of θ, this time with k fixed at $k = 10^5$ s^{-1} and for different noise rates. For each noise rate, there are two curves, one with and one without the oscillatory field. However, as explained in the text, these can only be properly distinguished for the case of weak noise (red curves).